

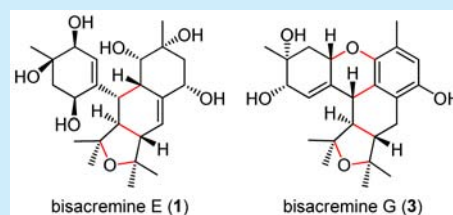
Bisacremines E–G, Three Polycyclic Dimeric Acremines Produced by *Acremonium persicinum* SC0105

Ping Wu, Jinghua Xue, Lei Yao, Liangxiong Xu, Hanxiang Li, and Xiaoyi Wei*

Key Laboratory of Plant Resources Conservation and Sustainable Utilization and Guangdong Provincial Key Laboratory of Applied Botany, South China Botanical Garden, Chinese Academy of Sciences, Xingke Road 723, Tianhe District, Guangzhou 510650, People's Republic of China

Supporting Information

ABSTRACT: Three dimeric acremines, bisacremines E–G (1–3), with an unusual carbon skeleton were isolated from cultures of the soil-derived fungus *Acremonium persicinum* SC0105. Their structures were elucidated by spectroscopic analysis, X-ray diffraction, and ECD/TDDFT computations. Compound 3 exhibited inhibitory effects on the production of TNF- α , IL-6, and NO in LPS-stimulated macrophages. A biogenetic pathway with a [4 + 2] cycloaddition as the key reaction is proposed for 1–3.



Meroterpenoids are hybrid natural products of both terpenoid and nonterpenoid origin.¹ They have attracted much attention due to their unusual structure features, wide range of bioactivities,¹ and interesting biosynthetic mechanisms.² Acremines are simple meroterpenoids, which comprise an isoprenyl unit linked to a six-membered C₇ tetraketide ring and can be defined as C₁₂ merohemiterpenoids.³ They have been all isolated from cultures of the *Acremonium* fungal species *A. byssoides*⁴ and *A. persicinum*,^{3,5} except that acremine S is produced by the fungus *Isaria felina* KMM 4639.⁶ Acremines A–F and H–T, 5-chlorinated acremines A and H, and spiroacremines A and B are monomers containing a single C₁₂ unit.^{3–6} Their structural diversity is arising from various O-based functionalities and different six-membered tetraketide rings. Acremine G, consisting of two C₁₂ units, is the first dimeric derivative and is generated from acremines A and B by a Diels–Alder reaction and successive oxidative coupling.^{4b} Its biomimetic total synthesis has been achieved.⁷ Acremines A–D and G–N inhibit sporangial germination of the phytopathogen *Plasmopara viticola*.⁴

In our previous investigation on bioactive metabolites of the soil-derived strain *A. persicinum* SC0105, we obtained four dimeric acremines, bisacremines A–D, which were postulated to be derived from the co-occurring new monomer acremine T by dehydration, oxidation, and successive carbocationic inter- and intramolecular coupling.³ In continuing our study on this strain, three new dimers (Figure 1), bisacremines E–G (1–3), with an unusual carbon skeleton were obtained, of which 3 demonstrated in vitro anti-inflammatory activity. Herein, we report the isolation, structure elucidation, and bioactivity of these compounds. The plausible biogenetic pathway of 1–3 with a [4 + 2] cycloaddition as the key reaction is also described.

The EtOAc-soluble fraction obtained from the EtOH extract of the solid cultures of *A. persicinum* SC0105³ was separated by

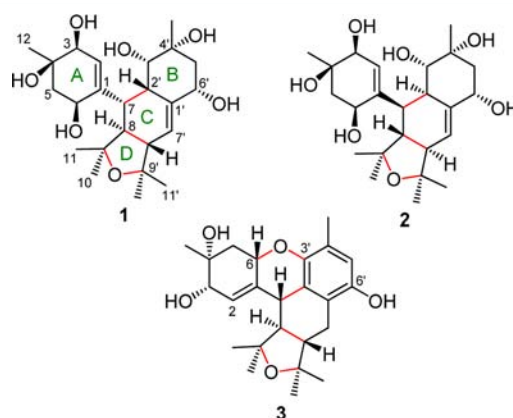


Figure 1. Structures of 1–3.

ODS CC followed by preparative HPLC to yield 1 as the major product and 2 and 3 as minor products.

Bisacremine E (1), obtained as colorless crystals (MeOH), was determined to have the molecular formula C₂₄H₃₈O₇ based on the HRESIMS. The ¹H and ¹³C NMR spectra (Table 1), with the aid of the HSQC spectrum, exhibited resonances for 10 methines, of which two were olefinic [δ_{H} 5.88 (1H, d, J = 2.7 Hz, H-2), 5.83 (1H, br s, H-7')]; δ_{C} 130.5 (C-2), 117.8 (C-7')] and four were oxygenated [δ_{H} 3.99 (1H, br d, J = 11.8 Hz, H-6'), 3.94 (2H, overlapped, H-3, H-6), 3.68 (1H, br s, H-3'); δ_{C} 70.0 (C-6'), 73.3 (C-3), 72.7 (C-6), 76.8 (C-3')], six quaternary carbons with two being olefinic [δ_{C} 141.5 (C-1'), 138.6 (C-1)] and four oxygenated [δ_{C} 83.0 (C-9), 80.4 (C-9'), 73.3 (C-4'), 71.8 (C-4)], six tertiary methyls, and two methylenes. The ¹H–¹H COSY spectrum (Figure 2) indicated the presence of fragments of H-2/H-3, H₂-5/H-6, H₂-5'/H-6',

Received: September 3, 2015

Published: September 24, 2015

Table 1. ^1H (600 MHz) and ^{13}C (150 MHz) NMR Data of 1–3 in CD_3OD^a

position	1		2		3	
	δ_{H} (multi, J, Hz)	δ_{C}	δ_{H} (multi, J, Hz)	δ_{C}	δ_{H} (multi, J, Hz)	δ_{C}
1		138.6		141.7		140.0
2	5.88 (d, 2.7)	130.5	5.49 (d, 2.2)	127.4	5.77 (dt, 4.7, 1.7)	122.0
3	3.94 (overlapped) ^b	73.3	3.98 (br s)	74.9	3.77 (br d, 4.7)	71.8
4		71.8		72.0		70.8
5	ax 1.86 (dd, 13.9, 5.0) eq 2.01 (dd, 13.9, 4.0)	41.9	ax 1.94 (dd, 13.9, 4.0) eq 2.00 (dd, 13.9, 5.0)	41.4	ax 1.86 (dd, 12.2, 9.2) eq 2.05 (br dd, 12.2, 5.9)	40.2
6	3.94 (overlapped) ^b	72.7	4.05 (t, 3.9)	68.9	4.77 (br dd, 9.2, 5.9)	77.0
7	2.63 (dd, 11.8, 6.7)	46.5	2.92 (overlapped) ^c	42.5	3.48 (d, 10.8)	41.3
8	2.96 (t, 11.8)	49.5	2.17 (t, 11.8)	49.8	2.38 (dd, 12.3, 10.8)	48.1
9		83.0		83.8		82.8
10	1.30 s	32.5	1.16 s	25.0	1.49 s	32.7
11	0.98 s	24.8	1.48 s	33.3	1.16 s	25.7
12	1.25 s	26.1	1.26 s	26.9	1.21 s	24.6
1'		141.5		142.8		120.3
2'	2.62 (br d, 6.7)	42.5	2.92 (overlapped) ^c	42.1		127.7
3'	3.68 (br s)	76.8	3.28 (br d, 9.4) ^c	76.2		145.9
4'		73.3		74.6		124.8
5'	ax 1.78 (t, 11.8) eq 1.83 (dd, 11.8, 5.0)	45.0	ax 1.65 (dd, 14.3, 4.0) eq 2.06 (dd, 14.3, 4.0)	43.0	6.42 s	115.6
6'	3.99 (br d, 11.8)	70.0	4.24 (t, 4.0)	74.5		149.5
7'	5.83 br s	117.8	5.77 (br s)	124.6	ax 2.22 (dd, 15.8, 12.8) eq 2.84 (dd, 15.8, 4.0)	25.2
8'	2.44 (br d, 11.8)	54.4	2.54 (d, 11.8)	54.3	2.11 (td, 12.3, 4.0)	50.9
9'		80.4		79.1		81.6
10'	1.08 s	24.7	1.28 s	29.4	1.23 s	25.0
11'	1.29 s	29.3	1.05 s	24.7	1.34 s	29.6
12'	1.21 s	25.2	1.17 s	27.7	2.08 s	15.9

^aChemical shifts (ppm) referenced to CD_3OD (δ_{H} 3.31; δ_{C} 49.0). ^bSignals in $\text{C}_5\text{D}_5\text{N}$: δ_{H} 4.38 (1H, t, $J = 4.3$ Hz, H-6), 4.36 (1H, br s, H-3). ^cSignals in $\text{C}_5\text{D}_5\text{N}$: δ_{H} 3.70 (1H, d, $J = 9.4$ Hz, H-3'), 3.46 (1H, dd, $J = 9.4, 7.2$ Hz, H-2'), 3.32 (1H, dd, $J = 11.8, 7.2$ Hz, H-7).

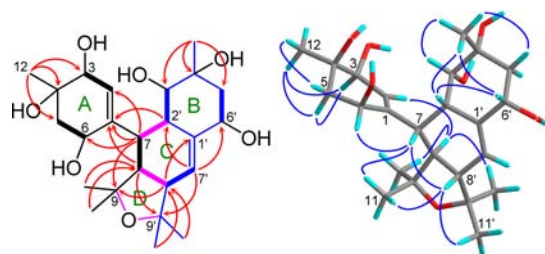


Figure 2. ^1H – ^1H COSY (bold lines), key HMBC (arrows), and key NOESY (curves) correlations of **1**. The 3D conformer represents the global energy minimum afforded by the theoretical conformational analysis.

and H-3'/H-2'/H-7/H-8/H-8'/H-7'. The HMBC spectrum (Figure 2) showed correlations from H₃-12 to C-3, C-4, and C-5, from H-7 to C-1, C-2, C-6, and C-9, from H-8 to C-1 and C-9', from H₃-10 and H₃-11 to C-8, from H₃-12' to C-3', C-4', and C-5', from H-7' to C-2', C-6', and C-9', from H-8' to C-1' and C-9, and from H₃-10' and H₃-11' to C-8'. These findings constructed a skeletal structure composed of two dihydrogenated acremine F^{4a,5} moieties, which were combined by direct connections between C-7/C-2' and C-8/C-8'. The downfield shifts of C-9 and C-9' (δ_{C} 83.0 and 80.4) and the unsaturation degree requirement supported C-9 being linked to C-9' via an O-bridge to form a tetrahydrofuran ring. The chemical shifts of C-3, C-4, C-6, C-3', C-4', and C-6' (Table 1) and the molecular formula indicated that these carbons all bear a hydroxy group to complete the gross structure of **1**.

The relative configuration of **1** was assigned by analysis of the NOESY data and ^1H NMR coupling constants. Key NOE interactions (Figure 2) observed between H-3/H-5_{ax}, H₃-12/H₂-5, H₃-12/H-3, H₃-12'/H-2', H₃-12'/H-3', H₃-12'/H-6', and H-2'/H-6', together with the proton coupling constant values, $J_{6,5\text{eq}} = 4.0$ Hz, $J_{6,5\text{ax}} = 5.0$ Hz, and $J_{6',5'\text{ax}} = 11.8$ Hz (Table 1), indicated that the three OH groups in each of rings A and B are oriented on the same side of the ring as those in the cyclohexenetriol moiety in acremines already obtained from this strain³ and H-2' is at the axial position in ring B and has the same orientation as 4'-CH₃ and H-6'. NOESY correlations of H-2/H-8, H₃-10 and H₃-10'/H-8, H-6/H-7, H₃-11/H-7, H-7/H-8', and H₃-11 and H₃-11'/H-8', in combination with the large proton coupling value, $J_{7,8} = J_{8,8'} = 11.8$ Hz, revealed that H-7, H-8, and H-8' are all at axial positions and H-7 and H-8' are oriented on the same side of ring C while H-8 is on the opposite side. The *cis* relationship between H-7 and H-2' was suggested by the $J_{7,2'}$ value (6.7 Hz), which was smaller than the *trans* axial–axial coupling. These structural conclusions were highly consistent with the lowest energy conformer (Figure 2) generated from the theoretical conformational analysis using the described method.³

As the six-membered tetraketide (methylcyclohexenetriol) ring in the acremines previously obtained from this strain has the 3*S*,4*R*,6*S* configuration,³ it is reasonable to consider that rings A and B in **1** also have this stereochemistry. Accordingly, the 2'*S*,3*S*,3'*S*,4*R*,4'*R*,6*S*,6'*S*,7*R*,8*S*,8'*S* configuration is assignable to **1**. The structure, including the stereochemistry, was finally confirmed by X-ray analysis (Figure 3).⁸

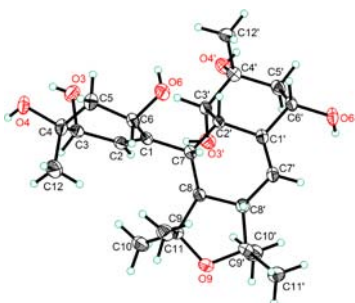


Figure 3. ORTEP drawing of **1** obtained by X-ray analysis.

Bisacremine F (**2**) was obtained as a white powder. Its molecular formula was determined to be the same as that of **1** on the basis of the HRESIMS. Analysis of the ^1H and ^{13}C NMR (Table 1), ^1H – ^1H COSY, HSQC, and HMBC data of **2** established a gross structure identical to that of **1**. Structural differences between **2** and **1** were found in the ^1H NMR and NOESY spectra. In the ^1H NMR spectrum of **2** in CD_3OD , the signal of H-3' appeared as a broad doublet at δ_{H} 3.28 with a large J value (9.4 Hz) consistent with a *trans* axial–axial coupling. In the NOESY spectrum of **2** in CD_3OD , NOE interactions were observed between H-3'/H-8 (δ_{H} 2.17), H-8/H-2 (δ_{H} 5.49), H-2/H-3', and H-3'/H-5'*ax* (δ_{H} 1.65) (Figure 4); and in the spectrum measured in $\text{C}_5\text{D}_5\text{N}$, correlations were

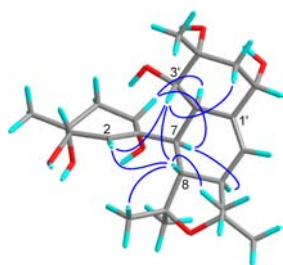


Figure 4. Key NOESY correlations (curves) of **2**. The 3D conformer represents the global energy minimum afforded by the theoretical conformational analysis.

also identified for H-6 (δ_{H} 4.55)/H-7 (δ_{H} 3.32), H-6/H-2' (δ_{H} 3.46), and H-7/H-8' (δ_{H} 2.51) (Figure 4); whereas the NOE of H-3'/H-2' was absent in both NOESY spectra. These facts evidenced that the chiral carbons in ring C, including C-2', in **1** are inverted in **2**. This structural conclusion was supported by the theoretical conformational analysis which provided the lowest-energy conformer (Figure 4) fully matching up with the above-mentioned NMR data. Therefore, **2** was characterized to be the 2'*R*,7*S*,8*R*,8'*R* isomer of **1**.

Bisacremine G (**3**), isolated as a white powder, has the molecular formula $\text{C}_{24}\text{H}_{32}\text{O}_5$ as determined by the HRESIMS. The ^1H and ^{13}C NMR spectra (Table 1), in combination with the HSQC spectrum, showed that **3** is also a dimeric acremine with one of C_{12} units being the 7,8-dihydrogenated acremine F moiety as that of **1**. However, the ^1H and ^{13}C NMR data for the other C_{12} unit were quite different from those in **1**, in particular, the resonances for an aromatic methine [δ_{H} 6.42 (1H, s, H-5'); δ_{C} 115.6 (C-5')], a benzylic methyl [δ_{H} 2.08 (3H, s, H₃-12'); δ_{C} 15.9 (C-12')], and five aromatic quaternary carbons with two being oxygenated [δ_{C} 149.5 (C-6') and 145.9 (C-3')], which were absent in the spectra of **1**. Analysis of ^1H – ^1H COSY and HMBC data of **3** (Figure 5) enabled establishment

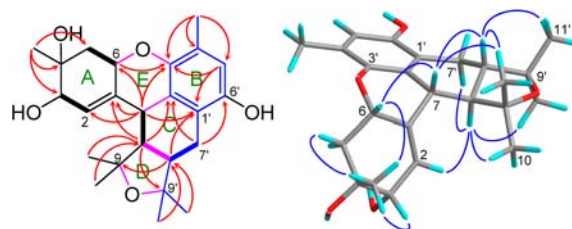


Figure 5. ^1H – ^1H COSY (bold lines), key HMBC (arrows), and key NOESY (curves) correlations of **3**. The 3D conformer is a representative of the dominant energy minima from the theoretical conformational analysis.

of a 2-isopentyl-5-methylhydroquinone moiety as the second C_{12} unit and constructed a pentacyclic structure. The presence of an O-bridge between C-6 and C-3' was supported by the downfield shift of C-6 (δ_{C} 77.0). In the NOESY spectrum of **3** (Figure 5), cross-peaks observed between H₃-12/H-6, H-6/H-7, H-7/H-8', H-2/H-8, and H-8/H-7'*ax* revealed the β orientation of 4-CH₃, H-6, H-7, and H-8' and α orientation of H-8 to assign the relative configuration as shown.

On the basis of the deduced relative configuration and biogenetic consideration, the absolute configuration of **3** was expected to be 3*S*,4*R*,6*S*,7*R*,8*S*,8'*S*. This assignment was supported by ECD/TDDFT calculations³ which provided a theoretical ECD spectrum well matching the measured spectrum (Figure 6). For reliable comparative analysis, the

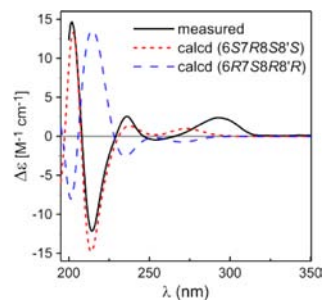


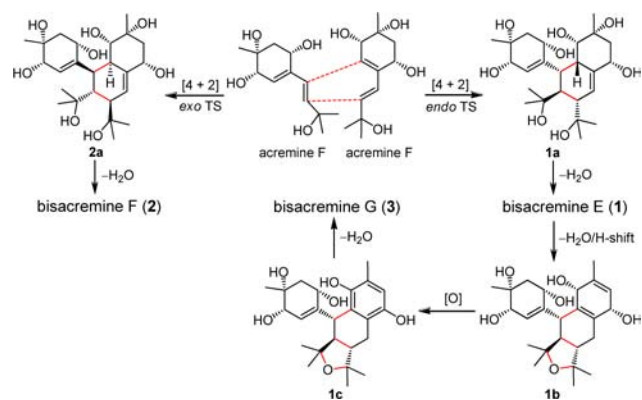
Figure 6. Comparison of the measured ECD spectrum of **3** with the $\omega\text{B97X}/\text{TZVP}$ calculated spectra of (3*S*,4*R*,6*S*,7*R*,8*S*,8'*S*)- and (3*S*,4*R*,6*R*,7*S*,8*R*,8'*R*)-**3** in MeOH.

6*R*,7*S*,8*R*,8'*R* isomer was also calculated and afforded a simulated ECD spectrum similar to the mirror image of the measured spectrum (Figure 6). Therefore, the complete structure of **3** was elucidated as depicted in Figure 1.

Compounds **1**–**3** represent a novel meroterpenoidal carbon skeleton and have an unprecedented tetracyclic or pentacyclic ring system. They are probably derived from acremine F, which was also obtained from this strain.³ A plausible route to **1**–**3** is shown in Scheme 1. In the biosynthesis, two molecules of acremine F undergo Diels–Alder cycloaddition⁹ to generate the *endo*-product **1a** (major) and *exo*-product **2a** (minor) as the key intermediates, which are dehydrated to yield **1** and **2**, respectively. Compound **3** is produced from **1** by dehydration, 1,3-H shift, oxidation, and further dehydration.

Compounds **1**–**3** were neither antibacterial against *S. aureus* nor cytotoxic against A549, MCF-7, and HepG2 cells. In the *in vitro* anti-inflammation assay,¹⁰ **3** exhibited dose-dependent inhibitory effects on the production of TNF- α , IL-6, and nitric oxide (NO) in LPS-stimulated RAW 264.7 macrophages. At 50 μM , it inhibited TNF- α , IL-6, and NO production by 80.1%,

Scheme 1. Plausible Biogenetic Pathway of 1–3



89.4%, and 55.7%, respectively. The inhibition was comparable to that of dexamethasone (inhibition rates at 50 μM : 78.0%, 92.6%, and 62.6%, respectively). However, the activity of **1** and **2** was weak at the same concentration (see the [Information](#)). The results suggested that the hydroquinone moiety is probably important for the anti-inflammatory activity of this group of compounds. The novel skeletal structure and noticeable activity may make **3** an attractive molecule for further chemical and biological investigation in order to discover new anti-inflammatory agents.

■ ASSOCIATED CONTENT

Supporting Information

The Supporting Information is available free of charge on the ACS Publications website at DOI: [10.1021/acs.orglett.5b02536](https://doi.org/10.1021/acs.orglett.5b02536).

X-ray crystallographic data for **1** (CIF)

Experimental section, computational details, 1D and 2D NMR spectra, and HRESIMS of **1–3** (PDF)

■ AUTHOR INFORMATION

Corresponding Author

*Tel: +86-20-3725-2538. E-mail: wxy@scbg.ac.cn.

Notes

The authors declare no competing financial interest.

■ ACKNOWLEDGMENTS

We thank Dr. X.-L. Feng, Instrumental Analysis & Research Center, Sun Yat-sen University, for X-ray diffraction analysis and Ms. Aijun Sun, South China Sea Institute of Oceanology, CAS, for HRESIMS and ECD measurements. This work was supported by an NSFC grant (No. 81172942) and a research project from the Bureau of Science and Technology of Guangzhou Municipality (Grant No. 201510010015).

■ REFERENCES

- (1) Geris, R.; Simpson, T. S. *Nat. Prod. Rep.* **2009**, *26*, 1063–1094.
- (2) Baunach, M.; Franke, J.; Hertweck, C. *Angew. Chem., Int. Ed.* **2015**, *54*, 2604–2626.
- (3) Wu, P.; Yao, L.; Xu, L.; Xue, J.; Wei, X. *J. Nat. Prod.* **2015**, *78*, 2161.
- (4) (a) Assante, G.; Dallavalle, S.; Malpezzi, L.; Nasini, G.; Burruano, S.; Torta, L. *Tetrahedron* **2005**, *61*, 7686–7692. (b) Arnone, A.; Nasini, G.; Panzeri, W.; de Pava, O. V.; Malpezzi, L. *J. Nat. Prod.* **2008**, *71*, 146–149. (c) Arnone, A.; Assante, G.; Bava, A.; Dallavalle, S.; Nasini, G. *Tetrahedron* **2009**, *65*, 786–791.

(5) Suciati; Fraser, J. A.; Lambert, L. K.; Pierens, G. K.; Bernhardt, P. V.; Garson, M. J. *J. Nat. Prod.* **2013**, *76*, 1432–1440.

(6) Yurchenko, A. N.; Smetanina, O. F.; Kalinovsky, A. I.; Pushilin, M. A.; Glazunov, V. P.; Khudyakova, Y. V.; Kirichuk, N. N.; Ermakova, S. P.; Dyshlovoy, S. A.; Yurchenko, E. A.; Afiyatullo, S. Sh. *J. Nat. Prod.* **2014**, *77*, 1321–1328.

(7) (a) Arkoudis, E.; Lykakis, I. N.; Gryparis, C.; Stratakis, M. *Org. Lett.* **2009**, *11*, 2988–2991. (b) Mehta, G.; Khan, T. B.; Kumar, Y. C. S. *Tetrahedron Lett.* **2010**, *51*, 5116–5119.

(8) Crystallographic data have been deposited at the Cambridge Crystallographic Data Centre under reference no. CCDC 1421019.

(9) (a) Stocking, E. M.; Williams, R. M. *Angew. Chem., Int. Ed.* **2003**, *42*, 3078–3115. (b) Kim, H. J.; Ruzsyczky, M. W.; Choi, S.-Y.; Liu, Y.-N.; Liu, H.-W. *Nature* **2011**, *473*, 109–112.

(10) (a) Wu, P.; Wu, M.; Xu, L.; Xie, H.; Wei, X. *Food Chem.* **2014**, *152*, 23–28. (b) Green, L. C.; Wagner, D. A.; Glogowski, J.; Skipper, P. L.; Wishnok, J. S.; Tannenbaum, S. R. *Anal. Biochem.* **1982**, *126*, 131–138.